HHS Public Access

Author manuscript

J Magn Reson Imaging. Author manuscript; available in PMC 2016 March 25.

Published in final edited form as:

J Magn Reson Imaging. 2012 February ; 35(2): 449–455. doi:10.1002/jmri.22839.

Assessment of Carotid Stenosis Using Three-Dimensional T2-Weighted Dark Blood Imaging: Initial Experience

Georgeta Mihai, PhD[1,2,*], **Marshall W. Winner, MD**[1], **Subha V. Raman, MD, MSEE**[1,2], **Sanjay Rajagopalan, MD**[1,2], **Orlando P. Simonetti, PhD**[1,2,3], and **Yiu-Cho Chung, PhD**[4]

1

2

3

4

Abstract

Purpose—To evaluate the use of a T2-weighted SPACE sequence (T2w-SPACE) to assess carotid stenosis via several methods and compare its performance with contrast-enhanced magnetic resonance angiography (ceMRA).

Materials and Methods—Fifteen patients with carotid atherosclerosis underwent dark blood (DB)-MRI using a 3D turbo spin echo with variable flip angles sequence (T2w-SPACE) and ceMRA. Images were coregistered and evaluated by two observers. Comparisons were made for luminal diameter, luminal area, degree of luminal stenosis (NAS-CET: North American Symptomatic Endarterectomy Trial; ECST: European Carotid Surgery Trial, and area stenosis), and vessel wall area. Degree of NASCET stenosis was clinically classified as mild (<50%), moderate (50%–69%), or severe (>69%).

Results—Excellent agreement was seen between ceMRA and T2w-SPACE and between observers for assessment of lumen diameter, lumen area, vessel wall area, and degree of NAS-CET stenosis ($r > 0.80$, $P < 0.001$). ECST stenosis was consistently higher than NASCET stenosis (48 ± 14% vs. 24 ± 22%, $P < 0.001$). Area stenosis (72 ± 2%) was significantly higher ($P < 0.001$) than both ESCT and NASCET stenosis.

Conclusion—DB-MRI of carotid arteries using T2w-SPACE is clinically feasible. It provides accurate measurements of lumen size and degree of stenosis in comparison with ceMRA and offers a more reproducible measure of ECST stenosis than ceMRA.

Keywords

dark blood MRA; atherosclerosis; carotid stenosis; MR angiography

Current guidelines regarding surgical management of carotid atherosclerosis are based on luminal stenosis severity and the presence of clinical symptoms. The two most common

*Address reprint requests to: G.M., Research Assistant Professor, Dorothy Davis Heart & Lung Research Institute, Room 110, 473 W 12th Ave., Columbus, OH 43210-1252. georgeta.mihai@osumc.edu.

methods used to measure carotid artery stenosis are derived from the North American Symptomatic Carotid Endarterectomy Trial (NASCET) and the European Carotid Surgery Trial (ECST) (1,2). Both were originally developed for use with digital subtraction angiography (DSA). Although both methods are well validated and have been proven to predict benefit after carotid endarterectomy in large clinical trials (1–4), neither is an ideal measure of plaque vulnerability, and both suffer from considerable variability even when applied within a single modality such as DSA or contrast-enhanced magnetic resonance angiography (ceMRA) (5–7). The NASCET method uses a “disease free” distal reference vessel segment which may underestimate the degree of stenosis due to tapering of the distal vessel. Furthermore, the NASCET technique does not account for positive remodeling, which has been shown to predict disease progression (8). On the other hand, the ECST method imputes the “normal” lumen diameter at the site of stenosis as the reference segment (Fig. 1, location E). This leads to variability with lumenographic techniques. The ECST method produces a consistently higher degree of stenosis than the NASCET method (9).

Dark blood (DB) MRA methodologies have the potential to measure carotid stenosis using either of these methods. Prior two dimensional (2D) iterations of this technique have suffered from partial volume artifacts, inadequate slice positioning, and prolonged imaging time (10,11). The use of double inversion recovery (DIR) for blood suppression, which is most effective with thin slices oriented perpendicularly to the direction of blood flow, poses challenges owing to the tortuosity of the carotids (12). Sampling Perfection with Application optimized Contrast using different flip angle Evolution (SPACE) is a recently developed single slab three dimensional (3D) turbo spin echo sequence with high sampling efficiency. There is intrinsic blood suppression in the readout direction allowing efficient coronal slab-orientation when imaging the carotid arteries.

In this study we propose the use of a T2-weighted SPACE sequence (T2w-SPACE) to assess carotid stenosis via several methods and compare its performance to ceMRA.

MATERIALS AND METHODS

Subject Population

The study was approved by our institution’s Human Subjects Committee and was in compliance with HIPAA. Fifteen patients with carotid atherosclerosis disease (9 male; age range: 49–83 years; 67.5. ± 10.2 years) with normal kidney function and ≥40% carotid stenosis confirmed by clinically indicated duplex ultrasonography or invasive angiography were prospectively enrolled for inclusion in the study. Written informed consent was obtained from all subjects prior to imaging.

MRI Technique

All imaging procedures were performed with a 1.5 T 32-channel whole-body MRI scanner (MAGNETOM Avanto, Siemens Healthcare, Erlangen, Germany) with a maximum gradient amplitude of 45 mT/m and a slew rate of 200 mT/m/msec. A 4-channel (two right and two left elements) phased array carotid coil (Machnet, The Netherlands) was used for signal reception. To avoid patient movement during the study, the head of the subject laid on top of

a vacuum mattress (Vac-Lok Cushions, MEDTEC, Orange City, IA), which was wrapped around the carotid coils placed on the sides of the upper neck. Removal of air with in-room suction caused the mattress to form a “vacuum cast” around the subject’s head and neck, keeping the left and right elements of the imaging coil in place, while maintaining patient comfort. Subjects were asked not to chew or swallow during the exam.

Each patient underwent scanning using the same imaging protocol. Localization of the carotid arteries was obtained using a three-plane steady-state free precession (SSFP) localizer, followed by an axial stack of SSFP images extending from the base of the neck to beyond the carotid bifurcation. After localization, the patients underwent T2w-SPACE imaging with the imaging slab oriented in the coronal plane (so that blood flowing along the readout direction was optimally suppressed), followed by a pre- and postcontrast 3D gradient echo ceMRA. The postcontrast 3D ceMRA image set was obtained following a 0.02 mmol/kg body weight injection of gadopentetate dimeglumine (Magnevist, Bayer HealthCare Pharmaceuticals, Wayne, NY), administered at a rate of 2 mL per second. A test bolus (1–5 mL) of Magnevist was used to determine the optimal timing of the postcontrast acquisition.

T2w-SPACE Sequence—The T2w-SPACE sequence used here was originally proposed for rapid, 3D, T2-weighted imaging of the brain (13). This technique uses selective volume excitation (14) and nonselective refocusing pulses with variable flip angles tailored to a prescribed signal evolution. The design reduces echo spacing, allowing for long echo trains and high sampling efficiency. The T2w-SPACE and ceMRA sequence parameters used in this study are listed in Table 1.

Quantitative Measurements

For each subject the image datasets obtained from T2w-SPACE and ceMRA acquisitions were coregistered on a 3D postprocessing workstation (FUSION, Siemens Healthcare) After registration, multiplanar reconstructions (MPR) perpendicular to the long axis of the vessel were generated at four locations (Fig. 1A–D). All locations, including the location of maximal stenosis (location D), were selected by visualizing the vessel simultaneously in three orthogonal planes. If no luminal stenosis was identified, then no MPR image was created at location D. Hence, a total of three to four slices for both T2w-SPACE and ceMRA were generated for each vessel. In five cases the point of maximal stenosis was in the common carotid artery (CCA) and not the internal carotid artery (ICA). In these cases the stenosis image (Fig. 1, position D) was generated in the CCA.

Two independent observers (each with more than 3 years of cardiovascular and vessel wall MRI experience) performed manual measurements of lumen area by outlining the inner vessel wall border at each location on both T2w-SPACE and ceMRA MPR generated images. The shortest lumen diameter measurements were obtained at each location in both 3D image sets, while the outer border diameter and area was obtained only from the T2w-SPACE images. In lieu of an outer border diameter, an estimated original lumen diameter was taken from the ceMRA images. Additionally, in the MPR images from T2w-SPACE, plaque burden quantification in the form of vessel wall area was obtained by subtracting the

lumen area from the area obtained by outlining the outer vessel wall border. Luminal stenosis was calculated using the NASCET criteria, the ECST criteria, and the area stenosis method. The following formulas were used for the calculations (Fig. 1) (1,2,15):

$$NASCET\ percent\ stenosis = \frac{C - D}{C} * 100\% \quad [1]$$

$$ECST\ percent\ stenosis = \frac{E - D}{E} * 100\% \quad [2]$$

$$Area\ percent\ stenosis = \frac{Total\ vessel\ area - Lumen\ area}{Total\ vessel\ area} * 100\% \quad [3]$$

The NASCET stenoses were further classified as mild (<50%), moderate (50%–69%), and severe (>69%). Area stenosis was only calculated for the T2w-SPACE images.

Statistical Analysis

Statistical analysis was performed using Minitab (v. 15) and Stata SE (v. 8.1, StataCorp, College Station, TX). Quantitative measurements of lumen area, minimal lumen diameter, ECST stenosis, and NASCET stenosis were compared for each independent observer between T2w-SPACE and ceMRA. Interobserver variability for T2w-SPACE and ceMRA measurements was also assessed. Comparisons were performed using a two-sample *t*-test, calculation of the intraclass correlation coefficient *r*, and by the method of Bland and Altman, with a statistical significance set at $P < 0.05$.

RESULTS

Image acquisition was successful in all subjects and blood was well suppressed in T2w-SPACE images in all cases, as assessed by visual evaluation of the acquired images by the experienced observers. The 3D T2w-SPACE acquisition covered a region of interest measuring 200 mm in the cranial-caudal direction in 5.5 minutes. Of this 200 mm, ≈70 mm was within the sensitivity volume of the carotid imaging coils and provided interpretable data. A total of 107 MPR images were generated and analyzed from 30 carotid vessels. Missing images (13 total) were caused either by the lack of luminal stenosis (nine images) or the inability to clearly depict one of the carotid artery segments (four images). Quantitative measurements of lumen area, lumen diameter, and NASCET stenosis percentage showed good correlation between T2w-SPACE and ceMRA for each of the two observers, as well as good interobserver agreement ($r > 0.80$, $P < 0.001$ for all comparisons). Table 2 shows the reproducibility of measurements obtained within observers (for lumen area and diameter derived from MRA and T2w-SPACE) and between observers (for lumen area, lumen diameter, outer border diameter, and wall area derived using MRA and T2w-SPACE).

Bland–Altman plots of NASCET stenosis showed good correlation with no significant bias between T2w-SPACE and ceMRA for both observers (Fig. 2A). When the NASCET stenoses were classified as mild, moderate, or severe, there was good agreement between the

ceMRA and T2w-SPACE for all 21 arteries evaluated. Using ceMRA as the "gold standard," the sensitivity and specificity of T2w-SPACE for the detection of a 50% stenosis was 75% and 100%, respectively, for both observers 1 and 2. The overall diagnostic accuracy was 86% for observer 1 and 95% for observer 2 (Fig. 4A). For ECST stenosis, good interobserver agreement was seen for T2w-SPACE ($r = 0.87$) but not ceMRA ($r = 0.48$) (Fig. 2B). There was average agreement when comparing ceMRA to T2w-SPACE for the measurement of ECST stenosis ($r = 0.69$). Regardless of imaging sequence, the ECST stenosis values were significantly higher than the NASCET values (48 ± 14% vs. 24 ± 22%; $P < 0.001$). The differences appeared most pronounced for stenoses of less than 50%. Area stenosis (72 ± 2%) was significantly higher than both NASCET and ECST stenosis ($P < 0.001$ for both). There was good interobserver agreement in the measurement of vessel wall area ($r > 0.85$, $P < 0.001$) using T2w-SPACE. Using a mean value from both observers, no relationship existed between the vessel wall area measured with T2w-SPACE and the luminal stenosis from ceMRA ($r = 0.22$; $P = 0.34$). Improved correlation with vessel wall area was seen for ECST stenosis ($r = 0.46$; $P = 0.04$) and area stenosis ($r = 0.60$; $P < 0.01$).

Figure 3 depicts sagittal and transverse MPR T2w-SPACE and ceMRA of a 69-year-old male patient. Note that T2w-SPACE clearly shows positive remodeling and significant atherosclerotic plaque with only mild luminal stenosis. The stenosis measurements were 0%, 45%, and 78% for the NASCET, ECST, and area stenosis methods, respectively.

DISCUSSION

The accurate delineation of carotid stenosis has important implications for patient management. Current clinical methods to assess carotid stenosis are luminal-based and although well validated, suffer from variability owing to assumptions in the calculation of stenosis. In this study we provide our initial experience with a T2w-SPACE approach and compare and contrast estimation of stenosis using this approach with traditional luminal-based measurements. Our results highlight well-known limitations and assumptions in the calculation of stenosis using lumenographic approaches such as ceMRA and the potential advantages of vessel wall imaging approaches such as T2w-SPACE.

Current clinical approaches for the quantification of carotid stenosis include NASCET, ECST, and area stenosis methods. In our small series, T2w-SPACE compared favorably with ceMRA, a clinically established modality, with an overall diagnostic accuracy of 91% for the categorization of NASCET stenosis severity. As such, our study suggests that in subjects with chronic kidney disease T2w-SPACE may provide a clinically viable alternative to ceMRA, avoiding the need for gadolinium-based contrast agents for the measurement of luminal stenosis.

Furthermore, T2w-SPACE demonstrated greater interobserver reproducibility than ceMRA for the determination of ECST stenosis. In keeping with prior studies, stenosis severity using ECST resulted in systematic overestimation compared to NASCET derived luminal stenosis (9). This was particularly true for stenoses under 50%, and most likely due to the use of the distal internal carotid artery, which is inherently smaller than the carotid bifurcation, as the reference vessel.

Area stenosis was much more severe than that measured by either the NASCET or ECST criteria, again consistent with previously reported results (16). The original NASCET and ECST methods are based on a linear calculation of stenosis, despite the circular form of a nonstenosed vessel. Using the area formula of a circle, Alexandrov et al (17) therefore suggested the "squared area method": ICA stenosis = 1 − [residual diameter]^2/[diameter of normal appearing distal ICA or estimated diameter at the site of the lesion]^2. Theoretically, both methods represent extreme estimations of the exact degree of stenosis. The linear methods are based on the assumption that there is no stenosis in any other orientation, while the squared methods postulate a corresponding grade of stenosis in all orientations. These difficult theoretical considerations are further aggravated by limitations of lumnal-based approaches such as DSA and ceMRA, which assume vessel wall diameters of reference segments. An important advantage of T2w-SPACE is delineation of the outer vessel wall, thus enabling calculation of percent stenosis in the setting of remodeling at the site of stenosis.

Vessel wall area, a surrogate of plaque burden commonly used in clinical trials of antiatherosclerotic therapy, was reproducible between observers. Furthermore, the 3D dataset acquired with T2w-SPACE would simplify longitudinal studies by allowing offline image registration, thus facilitating identical slice positioning, which is a known problem with 2D techniques (10). Interestingly, vessel wall area and plaque burden cannot be inferred from luminal stenosis alone. There was no correlation between vessel wall area and NASCET stenosis, and only a weak correlation with ECST or area stenosis.

Conventional 2D carotid plaque imaging is done with transverse orientation. Recently, it was shown that longitudinal views provide additional complementary information (18). The T2w-SPACE sequence always comes with longitudinal views of the vessels, thus reducing the need for slice repositioning and shortening scan times. The technique also provides several advantages over other dark blood 2D or 3D MRA techniques. T2w-SPACE is more efficient than previously reported 2D and 3D dark blood sequences used to image the carotid arteries in terms of speed and spatial coverage (19). Compared to SSFP based dark blood 3D techniques, T2w-SPACE is insensitive to magnetic field inhomogeneity and can be used at high field strengths (eg, 3 T) where improved signal-to-noise ratio favors higher spatial resolution imaging. The variable flip angle used in T2w-SPACE also reduces the specific absorption rate (SAR) relative to comparable 3D fast spin echo methods, an important consideration in high field imaging. Moreover, T2w-SPACE is an intrinsically dark blood technique—flowing spins dephase along the readout (frequency encoding) direction (20,21).

Despite the inherent advantages of T2w-SPACE, it is pertinent to mention some of the limitations with the approach. In 4 of the 26 vessels, image quality was inadequate to attempt measurement of stenosis. This was due to either patient movement or difficulty in properly positioning the carotid coils. The coverage area for both ceMRA and T2w-SPACE imaging is limited to about 70 mm by the carotid coils. Incomplete blood suppression due to nonlaminar flow at the carotid bulb has been reported, but this was not seen in this series of patients. Also, three cases were mis-classified with regard to clinical stenosis severity (mild, moderate, or severe) by observer 1 and one case by observer 2. Reviewing these cases

showed a very small actual difference in percent stenosis (mean 7.8%) with the misclassification being mainly due to the abrupt cutoff of the arbitrary categories (Fig. 4B).

In conclusion, dark blood MRI of the carotid arteries using the T2w-SPACE sequence is clinically feasible. It provides accurate measurements of the vascular lumen and degree of NASCET stenosis in comparison with ceMRA, and can be used to replace ceMRA in patients with kidney failure. It provides greater inter-observer reproducibility for the measurement of ECST stenosis than ceMRA due to direct visualization of the vessel wall. Finally, it provides reproducible measurements of vessel wall area and area stenosis, which may be of potential value in clinical trials.

References

1. European Carotid Surgery Trialists' Collaborative Group. MRC European Carotid Surgery Trial: interim results for symptomatic patients with severe (70–99%) or with mild (0–29%) carotid stenosis. Lancet. 1991; 337:1235–1243. [PubMed: 1674060]
2. North American Symptomatic Carotid Endarterectomy Trial Collaborators. Beneficial effect of carotid endarterectomy in symptomatic patients with high-grade carotid stenosis. N Engl J Med. 1991; 325:445–453. [PubMed: 1852179]
3. Executive Committee for the Asymptomatic Carotid Atherosclerosis Study. Endarterectomy for asymptomatic carotid artery stenosis. JAMA. 1995; 273:1421–1428. [PubMed: 7723155]
4. Barnett HJ, Taylor DW, Eliasziw M, et al. Benefit of carotid end-arterectomy in patients with symptomatic moderate or severe stenosis. North American Symptomatic Carotid Endarterectomy Trial Collaborators. N Engl J Med. 1998; 339:1415–1425. [PubMed: 9811916]
5. JMUK-I, Graves MJ, Cross JJ, et al. Internal carotid artery stenosis: accuracy of subjective visual impression for evaluation with digital subtraction angiography and contrast-enhanced MR angiography. Radiology. 2007; 244:213–222. [PubMed: 17507721]
6. U-King-Im JM, Trivedi RA, Cross JJ, et al. Measuring carotid stenosis on contrast-enhanced magnetic resonance angiography: diagnostic performance and reproducibility of 3 different methods. Stroke. 2004; 35:2083–2088. [PubMed: 15243149]
7. Staikov IN, Arnold M, Mattle HP, et al. Comparison of the ECST, CC, and NASCET grading methods and ultrasound for assessing carotid stenosis. European Carotid Surgery Trial. North American Symptomatic Carotid Endarterectomy Trial. J Neurol. 2000; 247:681–686. [PubMed: 11081806]
8. Saam T, Hatsukami TS, Takaya N, et al. The vulnerable, or high-risk, atherosclerotic plaque: noninvasive MR imaging for characterization and assessment. Radiology. 2007; 244:64–77. [PubMed: 17581895]
9. Rothwell PM, Gibson RJ, Slattery J, Sellar RJ, Warlow CP. Equivalence of measurements of carotid stenosis. A comparison of three methods on 1001 angiograms. European Carotid Surgery Trialists' Collaborative Group. Stroke. 1994; 25:2435–2439. [PubMed: 7974586]
10. Balu N, Kerwin WS, Chu B, Liu F, Yuan C. Serial MRI of carotid plaque burden: influence of subject repositioning on measurement precision. Magn Reson Med. 2007; 57:592–599. [PubMed: 17326176]
11. Saam T, Ferguson MS, Yarnykh VL, et al. Quantitative evaluation of carotid plaque composition by in vivo MRI. Arterioscler Thromb Vasc Biol. 2005; 25:234–239. [PubMed: 15528475]
12. Simonetti OP, Finn JP, White RD, Laub G, Henry DA. "Black blood" T2-weighted inversion-recovery MR imaging of the heart. Radiology. 1996; 199:49–57. [PubMed: 8633172]
13. Mugler JP 3rd, Bao S, Mulkern RV, et al. Optimized single-slab three-dimensional spin-echo MR imaging of the brain. Radiology. 2000; 216:891–899. [PubMed: 10966728]
14. Mugler, JP., 3rd; Brookeman, JR. Efficient spatially-selective single-slab 3D turbo-spin-echo imaging. Proc 12th Annual Meeting ISMRM; Kyoto. 2004.

15. Hankey GJ, Warlow CP. Symptomatic carotid ischaemic events: safest and most cost effective way of selecting patients for angiography, before carotid endarterectomy. BMJ. 1990; 300:1485–1491. [PubMed: 2115384]

16. Babiarz LS, Astor B, Mohamed MA, Wasserman BA. Comparison of gadolinium-enhanced cardiovascular magnetic resonance angiography with high-resolution black blood cardiovascular magnetic resonance for assessing carotid artery stenosis. J Cardiovasc Magn Reson. 2007; 9:63–70. [PubMed: 17178682]

17. Alexandrov AV, Bladin CF, Maggisano R, Norris JW. Measuring carotid stenosis. Time for a reappraisal Stroke. 1993; 24:1292–1296. [PubMed: 8362420]

18. Yu W, Underhill HR, Ferguson MS, et al. The added value of longitudinal black-blood cardiovascular magnetic resonance angiography in the cross sectional identification of carotid atherosclerotic ulceration. J Cardiovasc Magn Reson. 2009; 11:31. [PubMed: 19689816]

19. Balu N, Chu B, Hatsukami TS, Yuan C, Yarnykh VL. Comparison between 2D and 3D high-resolution black-blood techniques for carotid artery wall imaging in clinically significant atherosclerosis. J Magn Reson Imaging. 2008; 27:918–924. [PubMed: 18383253]

20. Hinks RS, Constable RT. Gradient moment nulling in fast spin echo. Magn Reson Med. 1994; 32:698–706. [PubMed: 7869891]

21. Jara H, Yu BC, Caruthers SD, Melhem ER, Yucel EK. Voxel sensitivity function description of flow-induced signal loss in MR imaging: implications for black-blood MR angiography with turbo spin-echo sequences. Magn Reson Med. 1999; 41:575–590. [PubMed: 10204883]

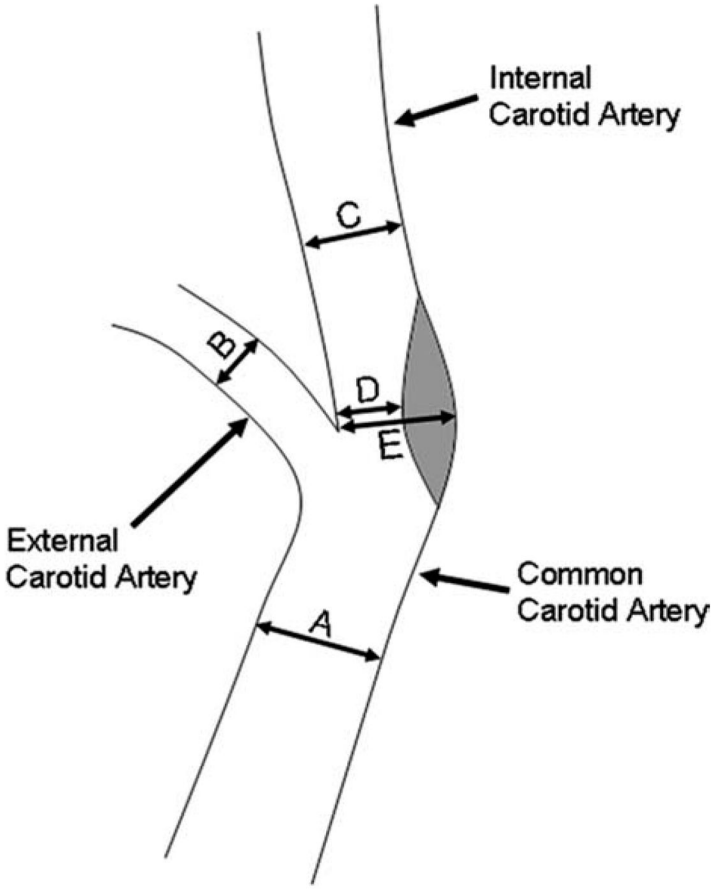

Figure 1.

Locations of measurements. A: Common carotid artery (CCA); B: External carotid artery (ECA); C: Internal carotid artery (ICA); D: Location of greatest stenosis when present; E: Outer vessel wall at the location of greatest stenosis when present. D and E were measured on the same image. NASCET stenosis calculated as (C–D)/C*100%. ESCT stenosis calculated as (E–D)/E*100%.

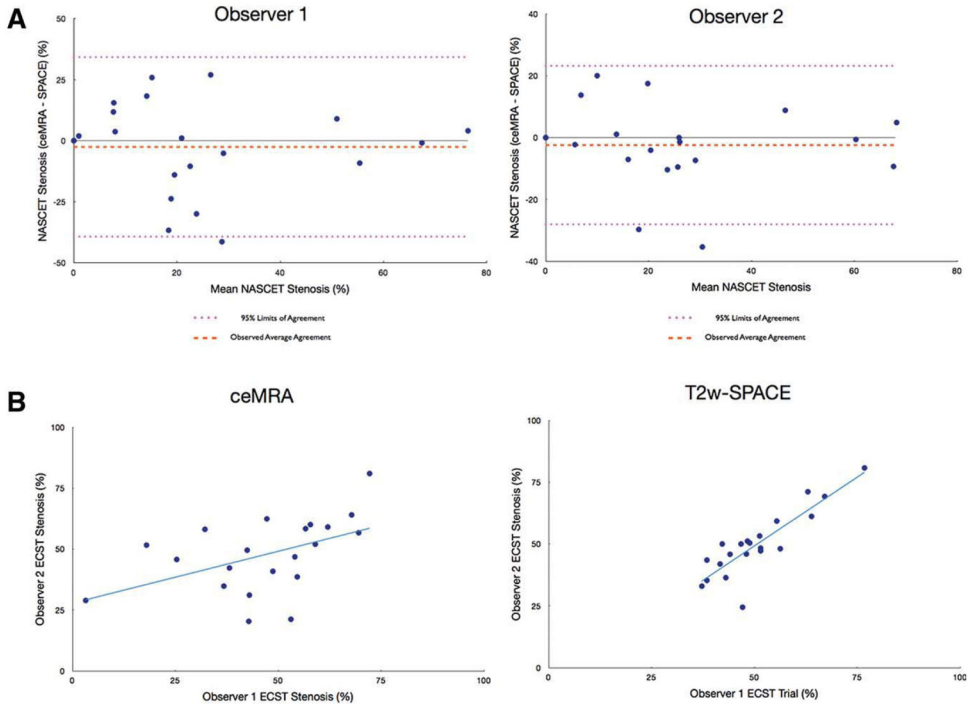

Figure 2.

A: Bland–Altman plots of stenosis severity percentages as assessed by NASCET criteria between ceMRA and T2w-SPACE for each observer. No significant bias is detected. **B**: Scatterplots displaying the interobserver reproducibility for the measurement of ECST stenosis using ceMRA (left) and T2w-SPACE (right) demonstrate improved correlation with T2w-SPACE.

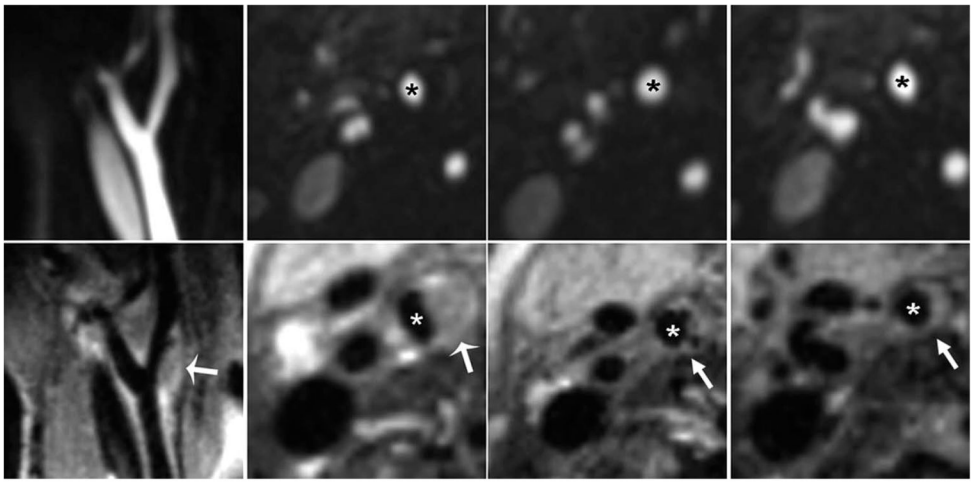

Figure 3.

A patient with moderate carotid artery stenosis as assessed by ceMRA (top row). The images from T2w-SPACE in the bottom row revealed that the plaque burden was worse than that showed in ceMRA. This was reflected in the stenosis measurements which were (average of both observers) 0%, 45%, and 78% for NASCET, ECST, and area stenosis, respectively. *Internal carotid artery; arrows point to plaque.

a

Observer 1

ceMRA \ SPACE	Mild	Moderate	Severe
Mild	17	0	0
Moderate	1	1	1
Severe	0	1	0

Observer 2

ceMRA \ SPACE	Mild	Moderate	Severe
Mild	17	0	0
Moderate	1	2	0
Severe	0	0	1

b

ceMRA (%)	T2w-SPACE (%)	Difference (%)
63	72	9
71	66	5
51	42	9
55	47	8
	Mean Difference	7.8

Figure 4.

A. NASCET Stenosis by Category for Each of the Two Observers and the Two Techniques.

B. ceMRA and T2w-SPACE Measurements in Vessels Where the Clinical Severity of Stenosis was Misclassified.

Table 1

Imaging Parameters

Imaging Parameters	T2W-SPACE	ceMRA
TR (ms)	1300	2
TE (ms)	119	1
Flip angle	Variable for refocusing pulses	30
Turbo factor	51	NA
Slice thickness (mm)	0.8	0.85
In-plane pixel size (mm^2)	0.8x0.8	0.8x0.8
IPAT factor	2	2
Echo Spacing	4.04	NA
Averages	2	1
Orientation	Coronal	Coronal
Number of slices	64	96
Total Scan time (minutes)	5.5	0.4-0.3

NA = not applicable; IPAT = parallel imaging acceleration factor.

Table 2

Agreement Analysis Between ceMRA and T2w-SPACE Techniques and the Two Independent Observers

		Pearson Correlation		2 sample t-test		
Observer 1		**r**	**p-value**	**Mean difference**	**95% CI**	**p-value**
MRA vs. SPACE	**Lumen Area**	0.993	<0.001	−0.001	(−0.044, 0.041)	0.953
	Lumen Diameter	0.869	<0.001	0.003	(−0.043, 0.049)	0.892
	NASCET	0.818	<0.001	−2.43	(−16.0, 11.1)	0.719
Observer 2		**r**	**p-value**	**Mean difference**	**95% CI**	**p-value**
MRA vs. SPACE	**Lumen Area**	0.963	<0.001	0.013	(−0.029, 0.056)	0.529
	Lumen Diameter	0.855	<0.001	0.020	(−0.027, 0.068)	0.394
	NASCET	0.908	<0.001	−0.81	(−15.5, 13.9)	0.912
Observer 1 vs. Observer 2		**r**	**p-value**	**Mean difference**	**95% CI**	**p-value**
MRA	**Lumen Area**	0.977	<0.001	−0.007	(−0.051, 0.036)	0.730
	Diameter	0.927	<0.001	−0.01	(−0.056, 0.036)	0.667
	NASCET	0.908	<0.001	0.24	(−13.4, 13.9)	0.972
SPACE	**Lumen Area**	0.982	<0.001	0.007	(−0.034, 0.048)	0.730
	Wall Area	0.875	<0.001	0.032	(−0.01, 0.074)	0.134
	Lumen Diameter	0.898	<0.001	0.001	(−0.046, 0.048)	0.963
	Outer Border Diameter	0.948	<0.001	0.022	(−0.035, 0.080)	0.440
	NASCET	0.912	<0.001	1.86	(−12.7, 16.4)	0.798
	ESCT	0.863	<0.001	0.81	(−6.6, 8.2)	0.827
	Area Stenosis	0.714	<0.001	1.33	(−4.8, 7.5)	0.663

Lumen area and diameter were measured for the point of maximal stenosis when present (position D, Fig. 1), as well as the internal, external, and common carotid arteries (positions A, B, and C, Fig. 1). Outer diameter, outer border diameter, and wall area were measured at the location of maximal stenosis (positions D and E, Fig. 1).